Absolute Characterization of Gravity Sag

H. Philip Stahl

NASA MARSHALL SPACE FLIGTH CENTER, HUNTSVILLE, AL 35812

ABSTRACT

G-release – defined as the knowledge uncertainty of a mirror's gravity-sag or the residual error between the mirror's predicted and actual on-orbit shape – is a critical error budget element for space telescopes. For a UV/Optical telescope, G-release needs to be less than 4 nm rms. Absolute metrology techniques developed for high-accuracy optical surface testing can be used for characterizing gravity-sag of space optics. This paper presents the importance of gravity sag for space optics and reviews methods for its compensation, characterization or correction.

Keywords: optical manufacture, optical test, space telescopes

1. INTRODUCTION

Per the National Research Council (NRC) ASTRO2010 Decadal Survey [1], 2012 NASA Space Technology Roadmaps and Priorities [2] and NASA's 2013 Enduring Quests Daring Visions [3], an advanced large-aperture ultraviolet/optical (UVO) space telescope is required to enable the next generation of compelling astrophysics and exoplanet science. To achieve UVO diffraction limited performance requires a telescope with a transmitted wavefront of approximately 30 nm rms or better. [4] An important parameter that must be controlled to achieve this performance is G-release error. For example, structural thermal optical performance (STOP) modeling for the Habitable Exoplanet Observatory telescope determined that to achieve diffraction limited performance of 400 nm, the primary mirror's gravity sag of approximately 20 micrometers rms must be characterized and compensated with an uncertainty of less than 4 nm rms. [5] One method for achieving this level of measurement precision is absolute calibration metrology.

2. G-RELEASE ERROR

G-release occurs because space mirrors are manufactured in a 1-G environment. During fabrication, mirrors experience self-weight deflection. But in the 0-G environment of space, there is no gravity and thus no self-weight deflection. The change in the mirror's shape from 1-G to 0-G is called G-release. Typically, G-release is most important for the primary mirror because it is the largest, lowest stiffness optical component in the telescope. Gravity Sag is also an important issue for ground-based telescopes – because pointing changes the mirror's orientation to gravity. Typically, ground telescopes use active primary mirror cells to compensate.

Self-weight deflection consists of two components: mount deflection and facesheet deflection. Mount deflection occurs due to the reaction or bending of the mirror substrate as it is accelerated by gravity against its opto-mechanical support mount. Mount deflection is commonly called Gravity Sag and is typically low-spatial frequency. Facesheet deflection occurs because space mirrors are typically lightweighted – leaving parts of the facesheet without support. These parts deflect slightly due to the acceleration of gravity against the vertical core ribs – and deflect more due to their response to the forces of grinding and polishing. Facesheet deflection is commonly called Quilting and is typically mid-spatial frequency. For the purposes of this paper, we will ignore facesheet deflection because methods to mitigate facesheet deflection or quilting are TRL-9. Proven mitigation approaches include designing the mirror with an appropriately thick facesheet and core pocket dimensions; pressurizing the mirror core cells to balance gravity during the fabrication process; or correcting with a small mechanical/ion polishing process.

Gravity-sag has been studied extensively since the 1960s. There are four possible mitigation approaches:

- Make the mirror as stiff as possible
- Support the mirror during fabrication in a 0-G configuration
- Characterize and remove G-sag from the mirror during the fabrication process
- Actively correct the mirror in space

2.1 Make the Mirror as Stiff as Possible

For any mirror, self-weight mount deflection gravity sag is proportional to geometry, mass density and mount interface.

$$1G\ Gravity\ Sag \sim C_{SP}\left(\frac{D^4}{t^3}\right)\rho_{AD} \sim 1/(2\pi\, f)^2,$$

where C_{SP} is mount support configuration constant [6], D is mirror substrate diameter, t is mirror substrate thickness, ρ_{AD} is mirror substrate mass areal density, and f is mirror substrate first mode frequency. Mount support configuration is important for two reasons: it determines the shape of the deformation and the amplitude (Figure 1). A complete discussion of mirror design methodology can be found in Yoder and Vukobratovich. [6]

Support Constant	C_{SP}	Factor of Reduced Deflection Compared to 3-Pt Support
Ring at 68% of Diameter	0.028	11
6 Points Equal Spaced at 68.1% of Diameter	0.041	8
Edge Clamped	0.187	1.5
3 Points, Equal Spaced at 64.5% of Diameter	0.316	-
3 Points, Equal Spaced at 66.7% of Diameter	0.323	~1
3 Points, Equal Spaced at 70.7% of Diameter	0.359	0.9
Edge Simply Supported	0.828	1/3
Continuous Support along the Diameter	0.943	1/3
"Central Support" (Mushroom or Stalk Mount; r = radius of stalk)	1.206	1/4
3 Points Equal Spaced at Edge	1.356	1/4

Figure 1: Mirror Deflection Amplitude Reduction as a function of Mount Support Configuration relative to a 3-point Mount. [6]

At the 4-meter size, it is impossible to make the mirror sufficiently stiff that its G-sag is < 4 nm rms. However, it is still important to make it as stiff as possible to minimize its gravity sag (because the smaller its amplitude, the easier it is to characterize and remove it from the 1-G metrology data).

To minimize gravity sag, make the mirror as thick as possible. For ULE® the state of art thickness is ~30 cm. Specialized abrasive waterjet machines can cut core elements as thick as 28 cm. [7] These elements can be frit bonded or low-temperature fused to form a mirror substrate. To make thicker mirrors, the Advanced Mirror Technology Development project successfully demonstrated a stack and seal process to manufacture a 40 cm thick test mirror. [8] For Zerodur®, Schott has demonstrated 42 cm thick substrates and they are working to produce 45 cm mirrors. [9] Other design elements that impact stiffness include: 1) face-sheet thickness; 2) whether or not the back of the mirror is open, closed, or partially closed and thickness of the back-sheet; 3) geometry of the core structure (i.e. iso-grid, rectilinear-grid, or hex-grid), pocket size, core wall thickness, etc. For example, hex-grid is more mass efficient but less stiff than iso-grid. Thus, hex is typically used for closed back mirrors (because the back sheet adds stiffness) and iso-grid is typically used for open back mirrors.

For the HabEx mission concept study, a Zerodur® mirror was designed that provided a balance between mass (for thermal stability) and stiffness (for mechanical stability). [5] The substrate has a flat-back geometry with a 42 cm edge thickness and mass of approximately 1400 kg. The mirror's free-free first mode frequency is 88 Hz and its mounted first mode frequency is 70 Hz. Mass is important because it provides thermal capacity for a thermally stable mirror. Additionally, mass allows for local stiffening of the substrate to minimize gravity sag. [10] The mirror substrate geometry and hexapod mount designs were optimized to produce as uniform as possible XYZ gravity sag deformation. The mirror is attached at three edge locations to a hexapod mount system. Figure 2 shows the baseline Zerodur® mirror's predicted 1-G PV (Peak-to-Valley) surface gravity sag in global telescope XYZ coordinate system (75.8 µm, 86.1 µm, 46.6 µm).

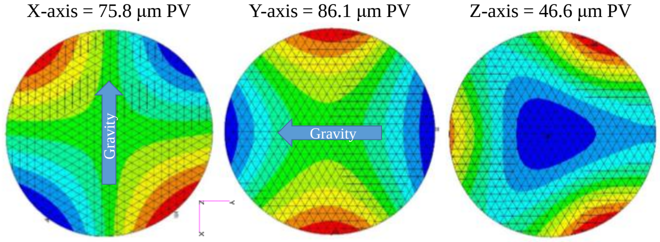

Figure 2: Primary Mirror Gravity Sag (PV surface deformation)

Please note, as discussed on Stahl 2020 [5], the baseline Zerodur® mirror design was not selected because it has the lowest gravity sag. Many different designs were considered, and at least one had a 4X smaller gravity sag. The baseline mirror design was selected based on an assessment of its performance, cost and fabrication risk.

Because it is not possible to design a large mirror with a sufficient stiffness to insure a small enough G-release for a UVO diffraction limited telescope, it is necessary to fabricate a 0-G mirror, i.e. a mirror that will have its required shape in space. This can be done by either supporting the mirror in a 0-G configuration or calculating and compensating for its G-sag during fabrication. Or, by designing the mirror to be correctable to achieve its required shape in space.

2.2 Support the Mirror during Fabrication in a 0-G Configuration

There are two methods for supporting a mirror in a 0-G configuration during fabrication and test: multipoint mount and air bag. For mid-quality mirrors, air bags are adequate. But for high-precision mirrors, multi-point mounts are preferred. The reason is that discrete mount points are more deterministic than a bag surface. An air bag exerts a force that is perpendicular to the mirror's back. If the mirror has a flat back, this is not a problem. But, if the mirror has a curved back, then the bag's 'off-loading' force vector is not parallel to the gravity vector, nor is it constant across the mirror. Also, lateral shear from stiction can impact local 'off-loading' force vectors. As a result, air bags can sometimes introduce rotationally symmetric errors, i.e. power or spherical. By contrast, the support points of a multiple-point mount can be placed at known locations with known orientations. And, they can be instrumented with force sensors to apply a precisely known upward force at each point.

Multi-point metrology mount technology was developed with NASA funding in the 1970s for the Large Space Telescope Program (Hubble). [6, 11, 12] The Hubble primary mirror's mounted 7.6 micrometer PV self-weight deflection was characterized to an accuracy of 1.4 nm rms using a 135 point metrology mount. [6, 13, 14] Figure 2 shows the Hubble primary mirror on its 135 point metrology mount. Figure 4 shows another 2.4-m mirror on a similar metrology mount.

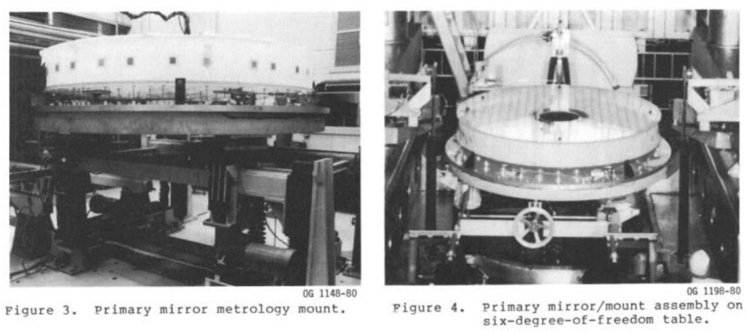

Fig 3: Hubble Primary Mirror on its Metrology Mount [14]

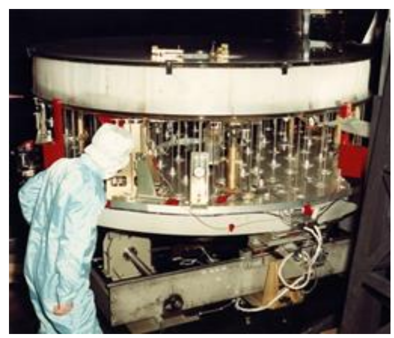
Fig 4: 2.4-m mirror on metrology mount [15]

Finally, the 1.4-m Kepler primary mirror was tested using both an air bag (Figure 5) and a 108 point metrology mount. The air bag was estimated to off-load gravity sag with an uncertainty of 5.6 nm rms. And, as shown in Figure 6, the difference between the air bag test and multi-point mount test was 16.4 nm rms (mostly spherical aberration). [16]

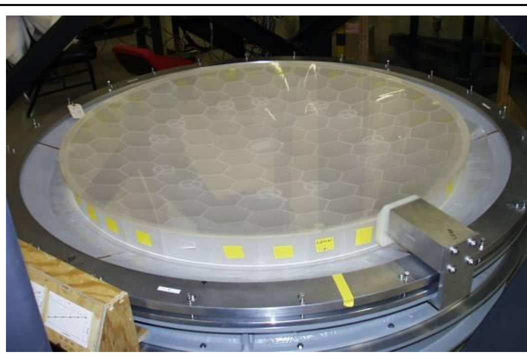
Fig 5: Kepler Primary Mirror on Air Bladder [16]

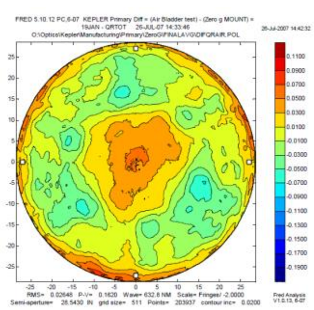
Fig 6: Difference between air bladder test and 108-point zero-g mount is 16.4 nm rms [16]

2.4 Characterize and remove G-sag from the mirror during the fabrication process

There are two methods to characterize a mirror's gravity-sag by test and analytically remove it during fabrication: vertical face-up/face-down test [16] and the horizontal rotation testing. [16 - 20]

2.4.1 Face-Up/Face-Down Gravity Orientation Test

The face-up/face-down test is simple. The mirror is tested on its flight mount. The mounted mirror's G-sag should be identical in the two orientations except for its polarity. Averaging the two measurements yields an estimate of the mirror's 0-G shape. Similarly, by taking half of the difference of these two measurements, one can estimate the mirror's gravity sag for comparison with prediction models. In the below equations, a gravity Z-vector of -1 points into the mirror's optical surface and produces a gravity sag that subtracts from the mirror's 0-G shape.

$$S(x,y)_{face-up} = S(x,y)_{G(0,0,0)} - S(x,y)_{G(0,0,-1)}$$

$$S(x,y)_{face-down} = S(x,y)_{G(0,0,0)} + S(x,y)_{G(0,0,1)}$$

$$0G\ Shape = S(x,y)_{G(0,0,0)} = \{S(x,y)_{face-up} + S(x,y)_{face-down}\}]/2$$

$$1G\ Sag = S(x,y)_{G(0,0,-1)} = \{S(x,y)_{face-up} - S(x,y)_{face-down}\}]/2$$

The Kepler primary mirror was assembled with a low thermal expansion flight mount (Figure 7) and characterized in a face-up/face-down gravity orientation test. The unpredicted difference between the air bag test and the up/down test was 18.4 nm rms (Figure 8). Of this error, 16.5 nm rms was symmetric (as is expected for an air bag test) and 6 nm rms was a 6-point bond pad pattern. [16] Additionally, when the finite element model predicted G-sag of 180 nm rms was compared with the measured up/down G-sag of 171 nm rms, they differed by 13.3 nm rms (Figure 9).

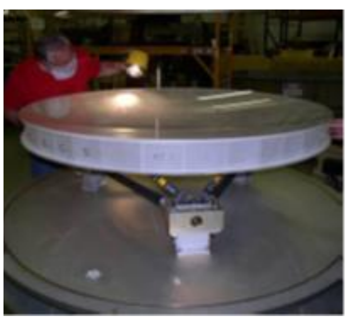

Fig 7: Kepler primary mirror on flight mount for face-up/face-down test. [16]

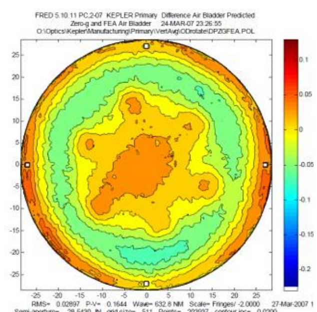

Fig 8: Difference between air bag test and up/down test. [16]

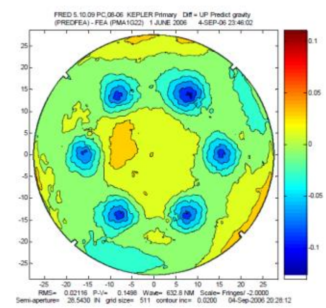

Fig 9: 13.3 nm rms difference between predicted and measured Gravity Sag. [16]

2.4.2 Horizontal Rotation Test

Rotation tests were originally developed to obtain an absolute measurement of a surface under test. Because interferometry is a relative measurement, the ability to manufacture precision surfaces is limited by knowledge of the reference wavefront (and internal interferometer errors). The purpose of an absolute test was to 'calibrate' the reference wavefront – allowing its error to be removed from the surface measurement. In the mid-1990s, Hughes Danbury Optical Systems (HDOS) developed a proprietary three flat test [17] to absolutely characterize the LIGO Pathfinder optic. [18] Concurrently, Evans and Kestner published the 'N-rotation' algorithm [19] where the interferometer measures a surface at N-rotation angles, i.e. N=3 (0°, 120°, 240°) or N=6 (0°, 60°, 120°, 180°, 240°, 300°). Averaging the measurements removes all test errors with angular dependence up to (N-1) Theta; and, all higher angular order errors that are not harmonics of N. So, an N=3 rotation test will remove 2-Theta errors (i.e. coma, secondary coma, tertiary coma, etc.; and, astigmatism, secondary astigmatism, tertiary astigmatism, etc.). However, N=3 case cannot remove trefoil. An N=6 rotation test is required to remove error terms up to 5-Theta (i.e. trefoil, tetrafoil, and pentafoil). It is important to note that the N-rotation test is 'blind' to rotationally symmetric errors. The HDOS algorithm solves this problem by adding an extra rotation angle. Appendix A provides an overview of historical absolute calibration metrology algorithms.

Because horizontal gravity sag is asymmetric, rotation tests can absolutely quantify gravity sag – thus allowing its removal from a surface measurement. For the below, the mirror's surface normal is assumed to point in the Z-direction and the Gravity vector is assumed to point in the -1 Y-direction. The measured shape consists of the mirror's 0-G shape decomposed into rotationally symmetric and rotationally asymmetric components and the mirror's gravity sag.

$$S(x,y,\theta_i)_{Horizontal} = \left[S(x,y)_{G(0,0,0)_{symmetric}} + S(x,y,\theta_i)_{G(0,0,0)_{asymmetric}}\right] + S(x,y,\theta = 0)_{G(0,-1,0)}$$

If a mirror is rotated in angles of theta around its surface normal that are symmetric with its flight mount, only the mirror's asymmetric component rotates. The gravity sag does not rotate, and obviously, neither does its rotationally symmetric component. Thus, averaging N-rotation measurements results in a measurement consisting of only the mirror's symmetric surface shape and its gravity-sag.

$$\frac{1}{N}\sum_{i=0}^{N-1} S\big(x,y,(\theta_i = 360(i/N))\big)_{Horizontal} = \left[S(x,y)_{G(0,0,0)_{symmetric}}\right] + S(x,y,\theta = 0)_{G(0,-1,0)}$$

While this is not particularly useful, if one back-rotates the measured data to theta = 0 before averaging, then instead of removing the mirror's asymmetric term, it is the Gravity Sag which is removed.

$$\frac{1}{N}\sum_{i=0}^{N-1} S\big(x,y,\{\theta_i = 0\big)_{Horizontal} = \left[S(x,y)_{G(0,0,0)_{symmetric}} + S(x,y)_{G(0,0,0)_{asymmetric}}\right]$$

As discussed above, the N-rotation method only removes asymmetric errors with angular dependence up to (N-1)-theta and higher angular order errors that are not harmonics of N. But as discussed in Appendix A, the HDOS algorithm overcomes this limitation by adding an extra rotation.

Each of the 18 JWST primary mirror segment assemblies (PSMAs) were testing using the rotation test method to an uncertainty of less than 10 nm rms. [20]

2.3 Actively Correct the Mirror in Space

While techniques exist to produce 0-G space mirrors via compensation or characterization, it is also possible to mitigate the risk of G-release error via an active mirror. Thus, while it is desirable to manufacture the primary mirror with as small of a G-release uncertainty as possible (TRL-9 capability is < 10 nm rms), an active primary mirror can easily correct 50 to 200 nm rms of error. For example, analysis of an alternative ULE® HabEx primary mirror indicates that 15 actuators can reduce low-order (i.e. astigmatic) G-release error by 20×, 25 can reduce G-release error by 40×, and 50 actuators can reduce G-release error by 100× (Figure 10). [21] Also, please note that active primary mirror technology is TRL-9. While they were never used, the Hubble PM (Primary Mirror) had 24 actuators to mitigate the risk of astigmatic G-release error. [6] And, the JWST PM has 18 actuators to mitigate the risk of segment radius matching error.

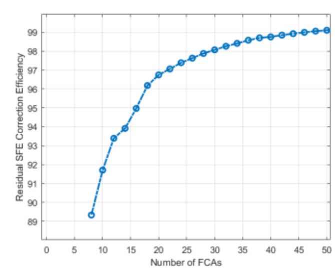

Fig 10: Correctability of alternative ULE® 4-m active primary mirror design as a function of actuators [21]

3. CONCLUSIONS

G-release is a critical error budget element for space telescopes. For a UV/Optical telescope, G-release needs to be less than 4 nm rms. Because it is not possible to design a large mirror with a sufficient stiffness to insure a small enough G-release for a UVO diffraction limited telescope, it is necessary to fabricate a 0-G mirror, i.e. a mirror that will have its required shape in space. This can be done by either supporting the mirror in a 0-G configuration or calculating and compensating for its G-sag during fabrication. Or, by designing the mirror to be correctable to achieve its required shape in space. There are two methods for supporting a mirror in a 0-G configuration during fabrication and test: multipoint mount and air bag. For mid-quality mirrors, air bags are adequate. But for high-precision mirrors, multi-point mounts are preferred. The reason is that discrete mount points are more deterministic than a bag surface. There are two methods to characterize a mirror's gravity-sag by test and analytically remove it during fabrication: vertical face-up/face-down test and the horizontal rotation testing. Finally, while it is desirable to manufacture the primary mirror with as small of a G-sag uncertainty as possible, G-release error can be mitigated with an active primary mirror.

APPENDIX: ABSOLUTE CALIBRATOIN

High-accuracy surface testing has been a subject of study since at least 1893 when Lord Rayleigh suggested both a liquid reference mirror and the basic principles of the three flat test. [22] Another early technique is the Ritchey-Common test (Shu, 1983 [23]). Unfortunately, liquid mirrors can be physically difficult to implement, and the Ritchey test is difficult to analyze. Thus, metrologists have developed various absolute calibration tests. Absolute calibration falls into four basic categories: Rotation Tests, Shear Test, Rotation-Shear Test, and Composite Averages. An excellent summary of absolute calibration techniques is given by Schultz and Schwider (1976) [24] and another by Burning (Optical Shop Testing, first and second editions). [25, 26] While the basics of absolute metrology remain constant, their implementation continues to advance with improvements in phase-measuring interferometer measurement precision and spatial sampling.

The rotation test and its extension the rotation-shear test are based upon the work of Schulz and Schwider (1967). [27] By inter-comparing three surfaces (A-B, A-C, and B^{180}-C), it is possible to calculate an exact (no interpolation) absolute calibration of a single diameter. This diameter is the line of symmetry about which surface B is inverted when it is moved from the bottom to the top, and the corresponding A, C surface diameters. Multiple diameters for each surface can be obtained by taking a fourth measurement (where one surface is rotated). (Figure A-1) The number of diameters (N) desired determines the rotation angle.

$$\theta = 2\pi \left[\frac{M}{N}\right] \qquad \text{where M and N are Prime to each other}$$

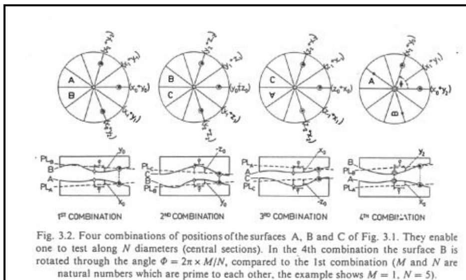

Fig A-1: Illustration of 4-rotation 3-flat test from Schulz and Schwider, 1976. [27]

Unfortunately, the three-surface rotation test is blind to angular errors which are harmonics of the rotation angle. To solve this problem and greatly increase the number of absolutely calibrated diameters, one can take a fifth (second rotation) measurement (Schulz, 1993). [28]

In Figure A-1, Shultz and Schwider used M = 1 and N = 5 for an rotation angle of 72 deg. But, 5 diameters is insufficient for modern applications. If, for example, one wants 1009 diameters, then two good rotation angles would be 71.00 degrees (N=199) and 100.97 (N=283). The reason that these are good rotation angles is that they are nearly prime to each other, thus their harmonics will be limited.

A similar technique for spherical surfaces, first suggested by Jensen (1973) [29] was demonstrated by Bruning (1974). [30] (Figure A-2) As with Shultz and Schwider's three surface test, the Jensen test is blind to harmonics of its rotation angle. The 180-degree rotation test illustrated in Figure A-2 only removes 1-theta errors such as coma. To remove 2-theta errors such as astigmatism requires four rotations of 90-degrees. To remove 3-theta errors such as trefoil requires six 60-degree rotations. An important feature of this test method is the cat's eye retro-reflection. This measurement allows the method to eliminate test setup symmetric and asymmetric errors from the part under test. Without this measurement, a rotation test can only calibrate the rotationally asymmetric errors. Fortunately, for the problem of characterizing gravity sag with the optic is in a horizontal test configuration, the gravity sag is asymmetric.

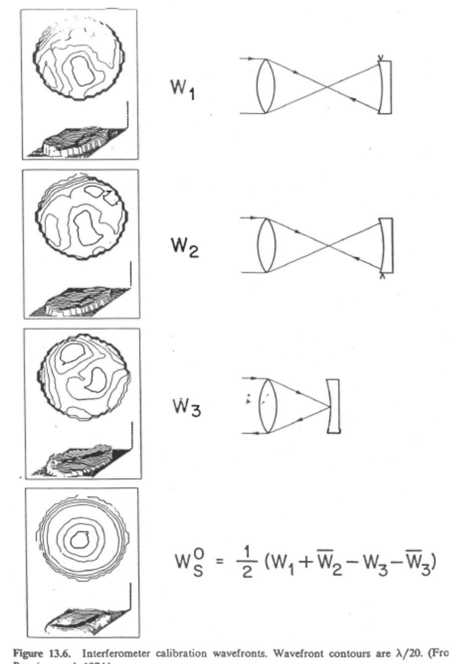

Fig A-2: From Bruning, Optical Shop Testing, 1978 [25]

In 1978, Parks described a back-rotation algorithm to calculate and remove asymmetric errors. [31] In the mid-1990s, Hughes Danbury Optical Systems (HDOS) developed a proprietary three flat test. [17, 18] And, Evans and Kestner published the 'N-rotation' algorithm [19] where the interferometer measures a surface at N-rotation angles, i.e. N=3 (0°, 120°, 240°) or N=6 (0°, 60°, 120°, 180°, 240°, 300°). Averaging the measurements removes all test errors with angular dependence up to (N-1) Theta; and, all higher angular order errors that are not harmonics of N. So, an N=3 rotation test will remove 2-Theta errors (i.e. coma, secondary coma, tertiary coma, etc.; and, astigmatism, secondary astigmatism, tertiary astigmatism, etc.). However, N=3 case cannot remove trefoil. An N=6 rotation test is required to remove error terms up to 5-Theta (i.e. trefoil, tetrafoil, and pentafoil).

A fundamental constraint of the rotation test is that its algorithms require the input data (and report the calibration results) in polar coordinates; while interferometers use cartesian coordinates (because their detectors are square arrays). Thus, data interpolation is required. One approach is to employ a global representation of the surface using Zernike polynomials (Parks, 1978 [31]; FritZ, 1982 [32, 33]) or Fourier expansion (Primak, 1988 [34]). Another method is to use local interpolation and a 2D least-squares fit (LSF) to solve the system of equations (Eisner, et ci., 1994 [35]; Schulz and Grazanna, 1992 [36], Grzanna, 1994 [37]). A completely different approach for obtaining cartesian calibration data is to use a shear test (Stahl, 1988 [38]) or rotation-shear test (Grazanna and Schulz, 1990 [39]). It is the fidelity of data interpolators that limits the uncertainty of rotation tests. For example, Zernike polynomial interpolation is a low pass filter – they ignore high-spatial frequency errors. And, grid interpolators can introduce registration errors that cause local surface shear. To achieve 2 nm rms calibration accuracy requires data set registration of approximately 1/10,000 of an aperture diameter.

The HDOS approach [17, 18] sought to overcome these limitations by implementing a method similar to Primak [34] in that the data is processed in Fourier space, but, instead of a 2D Fourier expanse, a circular harmonic transformation (CHT) was used. CHT was selected because each radial position is independent of all other radial positions, and by proper design of the rotation angles for which data is acquired, the circular data vector can be populated to any desired spatial frequency density. It is important to note that the HDOS approach is entirely consistent with Fritz. [32, 33]

The advantage of this approach is that it greatly reduces the required processing time and increases spatial frequency fidelity - even for densely sampled data. Based upon interpolation and a 1D FFT, it is much faster than conventional 2D expansion methods. And, because the FFT generates all angular frequency components simultaneously, an exact solution of the three surfaces is produced rather than a partial (low-order polynomial) approximation. The data processing flow is as follows. First, the measured data is interpolated from rectangular to polar coordinates. Next, it undergoes a 1D FFT with respect to the angular coordinate (CHT). Then, while in CHT space, the data is solved for even and odd angular frequency coefficients (Ai, 1993 [40]). Next the real and imaginary terms are combined into a complex frequency component for each of the surfaces. Performing an inverse FFT on each CHT space solution set produces a figure map in polar coordinates. Finally, these sets are interpolated back into cartesian coordinates. To avoid errors associated with the interpolator, the data was oversampled and an edge constraint window applied.

As with other rotation tests, the equations are undefined for angular frequencies which are harmonics of the rotation angle. At these angular frequencies the denominator term is zero. As a result, the solution of this set of equations contains voids in its angular spectrum. This problem is solved by taking a second rotation which is prime to the first and combining the results (Schulz, 1993 [28]).

The HDOS algorithm was used to test two 200 mm diameter LIGO Pathfinder Flat with a full-aperture accuracy of better than X/l000 (0.6 nm) rms. [18]

REFERENCES

1. Committee for a Decadal Survey of Astronomy and Astrophysics; National Research Council, New Worlds, New Horizons in Astronomy and Astrophysics, The National Academies Press, Washington, D.C., 2010.

2. NASA Space Technology Roadmaps and Priorities: Restoring NASA's Technological Edge and Paving the Way for a New Era in Space, NRC Report, 2012.

3. Enduring Quests Daring Visions, NASA Astrophysics Division, December 2013.

4. Stahl, H. Philip, Marc Postman and W. Scott Smith, "Engineering specifications for large aperture UVO space telescopes derived from science requirements", Proc. SPIE 8860, 2013, DOI: 10.1117/12.2024480

5. Stahl, H. Philip, Gary Kuan, William Arnold Sr., Thomas Brooks, J. Brent Knight, Stefan Martin, "Habitable-Zone Exoplanet Observatory (HabEx) baseline 4-m telescope: systems-engineering design process and predicted structural thermal optical performance", JATIS 20034R (2020)

6. Yoder, Paul and Danial Vukobratovich, Opto-Mechanical Systems Design, Fourth Edition, Two Volume Set, CRC, 2015 ISBN-10: 1439839778

7. Egerman, et. al., "Status of the Advanced Mirror Technology Development (AMTD) phase 2 1.5m ULE mirror", Proc. SPIE. 9575, Optical Manufacturing and Testing XI, 95750L. (August 27, 2015) doi: 10.1117/12.2188566

8. Stahl, H. Philip, "Advanced ultraviolet, optical, and infrared mirror technology development for very large space telescopes," J. Astron. Telesc. Instrum. Syst. 6(2) 025001 (23 May 2020) https://doi.org/10.1117/1.JATIS.6.2.025001
9. Westerhoff, Thomas, and Tony Hull, “Production of 4 m diameter Zerodur® mirror substrates”, HabEx White Paper Contribution, 2018.
10. Arnold, William R, H. Phillip Stahl, "Influence of core and hexapod geometry, and local reinforcement on the performance of ultra lightweight ULE mirror," Proc. SPIE 10743, Optical Modeling and Performance Predictions X, 107430B (17 September 2018); doi: 10.1117/12.2326017
11. Hall, H.D., Problems in adapting small mirror fabrication techniques to large mirrors, Optical Telescope Technology Workshop, April 1969, NASA Report SP-233, 1970.
12. Montagnino, R. Arnold, D. Chadwick, L. Grey, G. Rogers, "Test And Evaluation Of A 60-Inch Test Mirror," Proc. SPIE 0183, Space Optics II, (27 September 1979);
13. Krim, Michael H., "Metrology Mount Development And Verification For A Large Spaceborne Mirror," Proc. SPIE 0332, Advanced Technology Optical Telescopes I, (4 November 1982);
14. Montagnino, Lucian A., "Test And Evaluation Of The Hubble Space Telescope 2.4-meter Primary Mirror," Proc. SPIE 0571, Large Optics Technology, (21 February 1986)
15. https://www.hexagonkh9.com/blog/2019/1/19/hexagon-looked-at-the-earth-the-hubble-looked-at-the-stars
16. Zinn, John W., George W. Jones, "Kepler primary mirror assembly: FEA surface figure analyses and comparison to metrology," Proc. SPIE 6671, Optical Manufacturing and Testing VII, 667105 (14 September 2007)
17. Zolcinski-Couet, Marie-Christine, Joseph A. Magner, David A. Zweig, “Absolute calibration of flats for densely sampled data”, Proc. SPIE 2536, Optical Manufacturing and Testing, (8 September 1995); doi: 10.1117/12.218463
18. Robert Paul Bourgeois, Joann Magner, H. Philip Stahl, "Results of the calibration of interferometer transmission flats for the LIGO Pathfinder optics," Proc. SPIE 3134, Optical Manufacturing and Testing II, (1 November 1997); doi: 10.1117/12.295121
19. Evans, Chris J., and Robert N. Kestner, “Test optics error removal”, Applied Optics, Vol.35, No.7, pp.1015-21, 1 March 1996.
20. Stahl, H. Philip, et. al., “Survey of interferometric techniques used to test JWST optical components”, SPIE Proceedings 7790, 2010, DOI:10.1117/12.862234
21. Kissil, Andy “SFE Correction for HabEx Primary Mirror”, 12 July 2018
22. Rayleigh, Nature, Vol.48, pp.148, 1893
23. Shu, Ker Li, “Ray-trace analysis and data reduction methods for the Ritchey-Common test”, Applied Optics, Vol.22, pp.1876-86, 1983.
24. Schultz, G., and J. Schwider, “Interferometric Testing of Smooth Surfaces”, Progress in Optics XIII, pp.119-26, Wolf, North-Holland Publishing Co., 1976
25. Bruning, J. H., “Fringe Scanning Interferometers”, Optical Shop Testing, Malacara, Wiley and Son’s, 1978.
26. Greivenkamp, J. E., and J. H. Bruning, “Phase Shifting Interferometry”, Optical Shop Testing, Second Edition, Malacara, Wiley and Son’s , 1992.
27. Schultz, G., and J. Schwider, Applied Optics, Vol.6, pp.1077, 1967.
28. Schulz, Gunter, “Absolute flatness testing by an extended rotation method using two angle of rotation”, Applied Optics, Vol.32, No.7, pp.1055-59, 1 March 1993
29. Jensen, A. E., “Absolute Calibration Method for Laser Twyman-Green Wavefront Testing Interferometers” (abstract only), JOSA, Vol.63, pg.1313, 1973.

30. Bruning, J. H., et. al., “Digital Wavefront Measuring Interferometer for Testing Optical Surfaces and Lenses”, Applied Optics, Vol.13, pg.2693, 1974.

31. Parks, Robert E., “Removal of Test Optic Errors”, SPIE Proceedings 153, pp.56-63, 1978.

32. Fritz, Bernard S., “Absolute Calibration of an Optical Flat”, SPIE Proceedings 433, 1982.

33. Fritz, Bernard S., “Absolute Calibration of an Optical Flat”, Optical Engineering, Vol. 23, pp.379, 1984.

34. Primak, William, “Optical flatness standard II: reduction of interferograms”, SPIE Proceedings 954, pp.375-81, 1988

35. Elsner, K., A. Vogel, J. Garzanna, G. Shulz, “Establishing a flatness standard”, Applied Optics, Vol.33, No.13, pp.2437-46, 1 May 1994.

36. Schulz, G. and J. Grazanna, “Absolute flatness testing by the rotation method with optimal measuring error compensation”, Applied Optics, Vol.31, No.19, pp.3767-80, 1 July 1992.

37. Grzanna, Jurgen, “Absolute testing of optical flats at points on a square grid: error propagation”, Applied Optics, Vol.33, No.28, pp.6654-61, 1994

38. Stahl, H. Philip and Jay A. Tome, “Phase-measuring interferometry: performance characterization and calibration”, SPIE Proceedings 954, 1988

39. Grzanna, J. and G. Shulz, “Absolute testing of flatness standards at square-grid points”, Optics Communications, Vol.77, No.23, pp.107-12, 15 June 1990.

40. Ai, Chiayu, and James C. Wyant, “Absolute testing of flats by using even and odd function”, Applied Optics, Vol.32, No.25, pp.4698-4705, 1 September 1993